nation of paleomagnetic directions, on the other hand, does not require the normalization of remanent magnetization.
10. Y. Kok, *Earth Planet. Sci. Lett.* **166**, 105 (1999).
11. Y. Guyodo, P. Gaillot, J. E. T. Channell, *Earth Planet. Sci. Lett.* **184**, 109 (2000).
12. R. M. Negrini, K. L. Verosub, J. O. Davis, *Earth Planet. Sci. Lett.* **87**, 173 (1988).
13. K. Creer, N. Thouveny, I. Blunk, *Phys. Earth Planet. Int.* **64**, 314 (1990).
14. S. P. Lund, J. C. Liddicoat, K. R. Lajoie, T. L. Henyey, S. W. Robinson, *Geophys. Res. Lett.* **15**, 1101 (1988).
15. S. Levi, R. Karlin, *Earth Planet. Sci. Lett.* **92**, 219 (1989).
16. T. Yamazaki, N. Ioka, *Earth Planet. Sci. Lett.* **128**, 527 (1994).
17. J. W. Holt, J. L. Kirschvink, F. Garnier, *J. Geophys. Res.* **101**, 11655 (1996).
18. S. C. Cande, D. V. Kent, *J. Geophys. Res.* **100**, 6093 (1995).
19. Supplementary material, presented as a description or figure, is available on *Science* Online at www.sciencemag.org/cgi/content/full/295/5564/2435/DC1.
20. Inclination anomaly ΔI is defined as observed inclination minus the expected inclination from GAD. Usually, the sign of observed and dipole inclinations within a reversed polarity are inverted to give normal polarity equivalents.
21. D. Gubbins, P. Kelly, *Nature* **365**, 829 (1993).
22. C. L. Johnson, C. G. Constable, *Geophys. J. Int.* **131**, 643 (1997).
23. The Sint-800 paleointensity curve was established by integration of 33 relative paleointensity records from marine sediment cores of various regions. Because the paleointensity variation is globally synchronous, it can be used as a dating tool like the $\delta^{18}O$ stratigraphy.
24. M. A. Celaya, B. M. Clement, *Geophys. Res. Lett.* **15**, 52 (1988).
25. A major shift in climatic changes from the obliquity to eccentricity periodicities occurred at about 900 ka, which is known as the mid-Pleistocene transition (*31*). A shift of the dominant frequency in k is observed accordingly in this core. This suggests the validity of the age control in the Matuyama Chron on the basis of magnetostratigraphy.
26. N. Teanby, D. Gubbins, *Geophys. J. Int.* **142**, 563 (2000).
27. M. Hyodo, *J. Geomag. Geoelectr.* **36**, 45 (1984).
28. L. Tauxe, T. Pick, Y. S. Kok, *Geophys. Res. Lett.* **22**, 2885 (1995).
29. M. R. Rampino, *Geology* **7**, 584 (1979).
30. H.-U. Worm, *Earth Planet. Sci. Lett.* **147**, 55 (1997).
31. W. F. Ruddiman, M. E. Raymo, D. G. Martinson, B. M. Clement, J. Backman, *Paleoceanography* **4**, 353 (1989).
32. F. C. Bassinot *et al.*, *Earth Planet. Sci. Lett.* **126**, 91 (1994).
33. J. Laskar, *Icarus* **88**, 266 (1990).
34. D. Paillard, L. Labeyrie, P. Yiou, *EOS* **77**, 379 (1996).
35. We thank E. Usuda for help with the paleomagnetic measurements, Y. Yokoyama for discussion, and the crew and scientists aboard the IMAGES IV cruise for obtaining the core sample, in particular the late Dr. Luejiang Wang. Partly supported by the Superplume Project of the Ministry of Education, Culture, Sports, Science and Technology of Japan.

29 November 2001; accepted 21 February 2002

Sea-Level Fingerprinting as a Direct Test for the Source of Global Meltwater Pulse IA

P. U. Clark,[1] J. X. Mitrovica,[2]* G. A. Milne,[3] M. E. Tamisiea[2]

The ice reservoir that served as the source for the meltwater pulse IA remains enigmatic and controversial. We show that each of the melting scenarios that have been proposed for the event produces a distinct variation, or fingerprint, in the global distribution of meltwater. We compare sea-level fingerprints associated with various melting scenarios to existing sea-level records from Barbados and the Sunda Shelf and conclude that the southern Laurentide Ice Sheet could not have been the sole source of the meltwater pulse, whereas a substantial contribution from the Antarctic Ice Sheet is consistent with these records.

Records of global sea-level change provide important information on the dynamics and mass balance of glaciers and ice sheets and on the geophysical properties of Earth's interior. Moreover, the sea-level rise from melting ice sheets identifies an increase in the freshwater flux to the ocean that, if targeted at areas of deep water formation, may influence the oceanic thermohaline circulation and cause climate change. Ongoing rates of modern sea-level rise are 1 to 2 mm/year (*1*). By comparison, the Barbados record of sea-level rise during the last deglaciation identifies an extraordinary event, beginning ~14,200 years before the present (yr B.P.), when rates exceeded 40 mm/year (~20 m over ~500 years) (*2*), corresponding to a freshwater flux on the order of 0.5 Sv (1 Sv $\equiv 10^6$ m^3 s^{-1}). This meltwater pulse, mwp-IA, was a period of exceptionally rapid reduction of the global ice budget, which may have affected atmospheric and ocean circulation through the rapid decrease in ice topography and the large increase in freshwater flux to the ocean. Despite the importance of mwp-IA to the last deglaciation, the specific ice sheets responsible for the event remain uncertain (*3*). We propose a direct method for establishing the source of mwp-IA on the basis of geographic variations in the meltwater distribution (or, alternatively, sea-level rise) over the duration of the event.

The Laurentide Ice Sheet is commonly cited as the most likely source of mwp-IA primarily because of its large size (*4*). Specific evidence suggesting that this ice sheet was responsible for mwp-IA, however, is limited to deep-sea cores from the Gulf of Mexico and the Bermuda Rise that record a decrease in $\delta^{18}O$ subsequent to the onset of the event (*5*–*8*). Insofar as these sites record only meltwater draining through the Mississippi River, interpretation of the isotopic signal as recording mwp-IA necessarily implies that the meltwater pulse originated entirely from the southern sector of the ice sheet: Specifically, the Hudson Strait and Gulf of St. Lawrence also served as outlets for Laurentide meltwater, but records of freshwater flux through these outlets ($\delta^{18}O$ and ice-rafted debris) indicate insignificant discharge during mwp-IA (*9*, *10*). However, the argument for a lone southern Laurentide source for mwp-IA faces several serious objections (*11*). The Barents Sea and Fennoscandian Ice

Table 1. Normalized sea-level change for a source of mwp-IA in southern Laurentia. The scenarios "S. Laurentia" and "S. Laurentia–U" refer to cases where the (assumed instantaneous) melting in southern Laurentia is either proportional to ice height at the onset of mwp-IA (as in Fig. 1A) or uniform across the region, respectively. The scenarios "S. Laurentia–M1" and "S. Laurentia–M2" explore the sensitivity of the predictions to variations in the timing of melting. The M1 history assumes that the mwp-IA deglaciation occurred uniformly over a period of 1000 years rather than instantaneously, whereas the M2 history assumes that 20% of the melting took place over the first 400 years, followed by 60% over the next 200 years and the remaining 20% over the last 400 years.

Scenario	Normalized sea-level change					
	Barbados	Sunda Shelf	Tahiti	Bonaparte Gulf	Huon Peninsula	Argentine Shelf
S. Laurentia	0.74	1.12	1.28	1.03	1.08	1.34
S. Laurentia–U	0.74	1.12	1.29	1.04	1.09	1.33
S. Laurentia–M1	0.78	1.11	1.26	1.01	1.06	1.31
S. Laurentia–M2	0.77	1.11	1.26	1.01	1.06	1.31

[1]Department of Geosciences, Oregon State University, Corvallis, OR 97331, USA. [2]Department of Physics, University of Toronto, Toronto, Ontario M5S 1A7, Canada. [3]Department of Geological Sciences, University of Durham, Durham DH1 3LE, UK.

*To whom correspondence should be addressed. E-mail: jxm@physics.utoronto.ca

Sheets have also been proposed as the source for mwp-IA—the former because it was marine-based and thus susceptible to rapid collapse (*12*), and the latter because it was subject to atmospheric warming that began just before mwp-IA (*13*). However, both of these scenarios are also subject to a suite of counterarguments (*14*). Finally, although the Antarctic ice complex has been suggested as a source for the meltwater pulse (*3*), the evidence both for and against this view is not compelling. The ice sheet could have had sufficient mass to account for the discharge (*15*), and the excess ice volume in both the East and West Antarctic Ice Sheets would have been marine-based. Furthermore, various cores obtained from the Southern Ocean show evidence of a light peak in $\delta^{18}O$ at roughly the time of mwp-IA (*3, 16, 17*); however, these signals cannot be unambiguously linked to Antarctic discharge.

The rapid melting (or growth) of an ice complex will be accompanied by a sea-level change that departs significantly from a uniform, or eustatic, distribution (*18, 19*). The departure from eustasy is due primarily to self-gravitation in the surface load, although loading and rotational effects will also contribute (*20*). Any ice mass will draw ocean water toward it as a consequence of simple gravitational attraction. If this ice mass melts, then the gravitational "tide" will diminish and water will move away from the zone of ablation; however, the mean level of the global ocean will clearly increase. Accordingly, different scenarios for the origin of the meltwater pulse (e.g., melting from Laurentia, Antarctica, or the Barents Sea) should produce distinct sea-level signatures or "fingerprints" over the course of the mwp-IA event. Thus, global maps of these fingerprints, in combination with observational constraints on mwp-IA–induced sea-level change at a set of geographic sites, provide a robust method for determining the origin of the meltwater pulse or for testing specific hypotheses in regard to this origin.

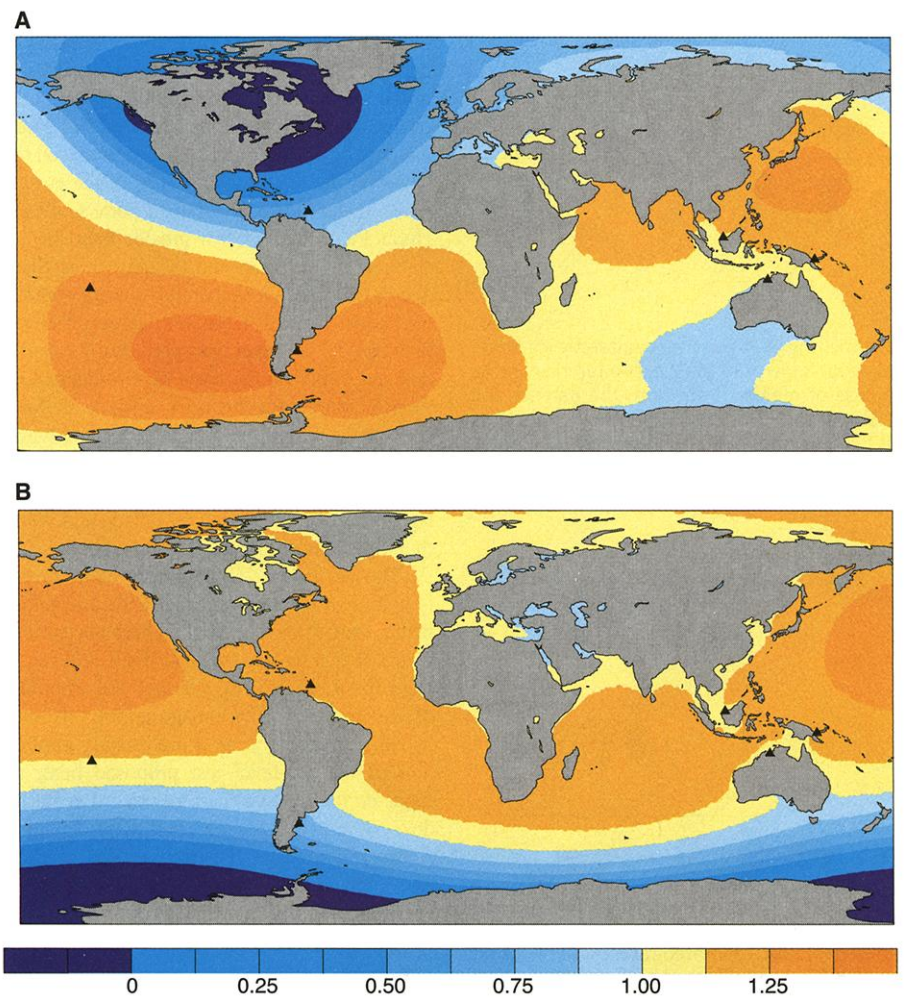

Fig 1. Normalized (dimensionless) sea-level change associated with melting from (**A**) the southern one-third of the Laurentide Ice Sheet and (**B**) West Antarctica, as they existed at the onset of the mwp-IA event. The predictions, which are described in detail in the text, assume that melting is proportional to ice height in this region relative to present-day values, as given by the ICE-3G deglaciation model (*21*). The predictions are normalized by the eustatic sea-level change; the color scale refers to fractions of this change. The small triangles denote the locations of six far-field sites considered in Table 1: (from left to right) Tahiti, Argentine Shelf, Barbados, Sunda Shelf, Bonaparte Gulf, and Huon Peninsula.

Figure 1A shows a prediction of the "normalized" sea-level pattern arising from a melting event on the southern one-third of the Laurentide Ice Sheet as it existed at the onset of the mwp-IA event (*21*). For purposes of comparison, Fig. 1B shows an analogous prediction for the case of a melting event confined to West Antarctica. These predictions are based on a new sea-level algorithm (*22*) that extends previous work (*23*) to include both an improved treatment of shoreline migration and perturbations in sea level due to contemporaneous, load-induced changes in the rotation vector of the Earth model. The predictions in Fig. 1 have been normalized by the eustatic value (total meltwater volume divided by the area of the ocean) during the mwp-IA event. Because these predictions represent the sea-level change after an instantaneous melting event, they are sensitive to the elastic properties of the Earth model (*24*); in contrast, the calculations are insensitive to the uncertain, and contentious, mantle viscosity structure. The predictions are also insensitive to variations in the global ice model adopted to define the melt geometry.

Consider Fig. 1A. The dark blue contouring in the vicinity of Laurentia indicates where sea level is predicted to fall according to this specific mwp-IA scenario. The remaining shades of blue denote areas where the predicted sea-level rise is smaller than the eustatic value. Because the mean change must equal the eustatic value, these areas must be balanced by zones where the sea-level rise exceeds this value (yellow-tan contours). Indeed, the maximum sea-level rise for this scenario, which occurs off the southwest coast of South America, is ~142% of the eustatic value. That is, if the mwp-IA event was associated with a eustatic sea-level rise of 20 m arising from melting in southern Laurentia, then sea level would actually fall off the Canadian coast and most of the U.S. east coast, it would rise by significantly less than 20 m in Europe, and it would rise by as much as 28.4 m in the southeast Pacific.

Determining the origin of mwp-IA is perhaps the optimal application of the sea-level test proposed here. The meltwater pulse was large (on the order of 20 m) and occurred over a remarkably short time scale (less than 1000 years), and this combination provides several advantages. The tectonic correction to the observed sea-level variation at sites commonly used for the analysis of sea-level change since the last glacial maximum is a fraction of a meter per 1000 years. Thus, uncertainties in this correction, which are a source of active debate in such analyses, are insignificant relative to geographic variations

in the sea-level maps associated with various mwp-IA melting scenarios (Fig. 1). We can also ignore sea-level changes driven by ocean thermal expansion over the mwp-IA time window, because these would also be on the order of 1 m (*25*).

In the near field of the late Pleistocene ice sheets, sea-level change over the course of the mwp-IA event will be strongly contaminated by the glacial isostatic adjustment (GIA) signal associated with prior ice mass variations. Accordingly, a comparison of sea-level fingerprints arising from the mwp-IA event (e.g., Fig. 1) with observational constraints would be most robust for so-called "far-field" data (*26*). The first row in Table 1 provides the values of the map in Fig. 1A at a set of six far-field sites widely discussed in the literature (the locations of these sites are shown as triangles in Fig. 1). The variation among the sites is clearly significant. As an example, if the mwp-IA event were due to a source entirely within southern Laurentia, then the sea-level rise at Tahiti and the Argentine Shelf would be ~73% and ~81% greater, respectively, than at Barbados. Thus, if the eustatic sea-level rise associated with the event were 20 m, then sea level would rise by 14.8 m at Barbados, 25.6 m at Tahiti, and 26.8 m on the Argentine Shelf.

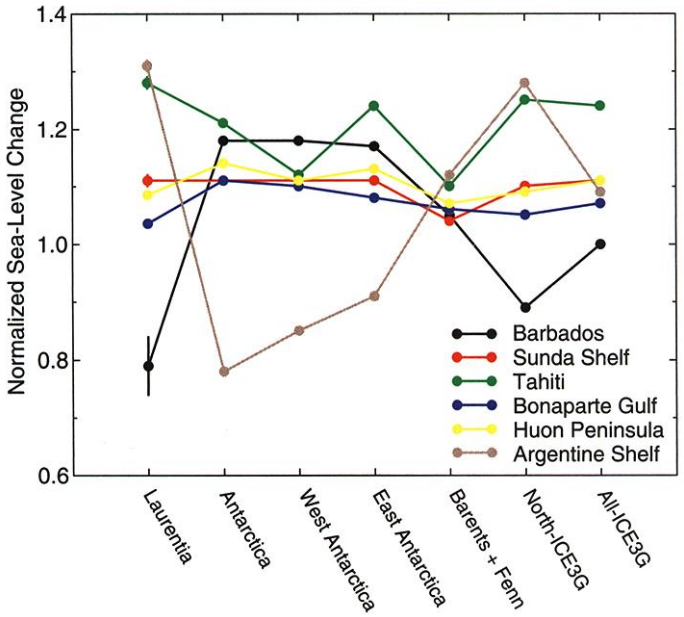

Fig. 2. Sea-level change (normalized by the eustatic value) at six sites for a series of seven distinct scenarios for the source of the mwp-IA event. "Laurentia" refers to a range of predictions generated by considering melting that is limited to one of the three sectors of the Laurentide Ice Sheet that drain meltwater toward the Mississippi, St. Lawrence, or Hudson Strait outlets, or a scenario in which the entire Laurentide Ice Sheet participates in the melting. (In the case of Barbados, melting from the southern Laurentian sector yields a sea-level rise ~75% of the eustatic value; see Table 1.) The next three cases refer to melting over the entire Antarctic Ice Sheet or the west and east portions of it, respectively. The sea-level fingerprint for West Antarctic melting is shown in Fig. 1B. "Barents + Fenn" represents the case of melting from both the Barents and Fennoscandian Ice Sheets. "North-ICE3G" refers to melting over all Northern Hemisphere ice sheets in the ICE-3G deglaciation model. The final case (All-ICE3G) extends this scenario to include all ice sheets within the ICE-3G model. In all cases, melting is assumed to be proportional to the ice heights at the onset of mwp-IA relative to present-day values.

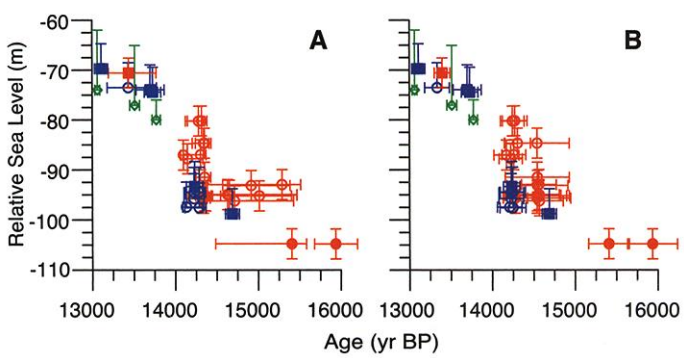

Fig. 3. Sea-level records from the last deglaciation; present sea level is at 0 m. The symbols represent U/Th ages on corals from Tahiti (green diamonds) (*27*), U/Th ages on corals from Barbados (solid blue squares) (*2*, *45*), calibrated radiocarbon ages from Barbados (open blue circles) (*45*, *46*), calibrated radiocarbon ages on non-mangrove samples from the Sunda Shelf (solid red circles) (*28*), calibrated radiocarbon ages on mangrove samples from the Sunda Shelf (open red circles) (*28*), and calibrated radiocarbon ages on a non-mangrove sample from the Sunda Shelf that is located ~100 km from other Sunda Shelf data shown (solid red squares) (*28*). U/Th ages are reported with 2σ error; calibrated radiocarbon ages are reported with 1σ error. In (**A**), we show sea-level records that include calibrated radiocarbon ages obtained from the intercept method (method A) of Calib 4.3 (*29*). We show only the calibrated age with its corresponding 1σ age range; additional calibrated 1σ age ranges may be possible. In (**B**), we show sea-level records that include calibrated radiocarbon ages from the probability distribution method (method B) of Calib 4.3 (*29*). We show only those calibrated ages that have the highest relative area under the probability distribution; additional calibrated ages with lower relative areas are possible.

In the remainder of Table 1 we consider the sensitivity of the predictions in Fig. 1A to variations in both the geometry and timing of the southern Laurentian melting scenario. None of the results are significantly different from those obtained using our original scenario, and we conclude that sea-level changes predicted for the six far-field sites are insensitive to these details.

In Fig. 2 we turn to a set of different scenarios for the origin of mwp-IA. For a given melting scenario, the geographic variation in the associated sea-level fingerprint is reflected in the scatter of the results along the "column" of the figure linked to the scenario. For example, any of the "Laurentian" scenarios lead to a sea-level rise within about 10% of the eustatic value at the Sunda Shelf, Bonaparte Gulf, and Huon Peninsula, ~30% greater than the eustatic value at Tahiti and the Argentine Shelf, and ~15 to 25% less than the eustatic value at Barbados. Note that the very large difference between the sea-level rises predicted for Barbados and Tahiti on the basis of a southern Laurentian source for mwp-IA disappears for a scenario in which the source is located within Antarctica (see also Fig. 1B). In this latter case, the sea-level rise on the Argentine Shelf will be significantly smaller than all others, and would thus be diagnostic of an Antarctic source.

The sea-level rise across mwp-IA is currently unknown for the Bonaparte Gulf, Huon Peninsula, and Argentine Shelf. There is clear evidence of a mwp-IA event in the Tahiti record from fossil corals (*27*), although the amplitude of the local sea-level change is not yet established. Accordingly, as a preliminary application of the sea-level test proposed here, we focus on the relative sea-level record at Barbados (*2*) and the Sunda Shelf (*28*). Figure 3 shows the relative sea-level record at these two sites and Tahiti (*27*) over a period that encompasses the mwp-IA event for two different dating schemes. The sharp sea-level rise evident between 14,500 and 14,200 yr B.P. represents the main phase of the meltwater pulse. Our goal is to establish from this data set a net change in sea level across mwp-IA (or some portion of the event) for each site, using a consistent time window. This effort is complicated by differences that arise when the original radiocarbon ages are calibrated using the two methods available in

the Calib 4.3 software (*29*). Nevertheless, data clustered at 13,500 yr B.P. and from 14,200 to 14,500 yr B.P. provide the required time window. Over this period, the Barbados data show a total sea-level rise of ~25 m (from ~ –98 m to ~ –73 m). The Sunda Shelf data suggest the same sea-level rise (from ~ –95 m to ~ –70 m) for this time window; however, this constraint is less robust (*30*).

If the source of mwp-IA was solely southern Laurentia, then a sea-level rise of 25 m at Barbados would have been accompanied by a rise of 38 m at the Sunda Shelf (Table 1). If we accept the validity of the observational constraint at the Sunda Shelf (of 25 m; Fig. 3), then this scenario appears to be ruled out (*31*). From Fig. 2, the smallest difference between Barbados and the Sunda Shelf for any (entirely) Laurentian source of mwp-IA is 30%, and in this case a sea-level rise of 25 m at Barbados would map into a sea-level change of ~33 m at the Sunda Shelf. This variation is at the upper bound of the sea-level change allowed by the data in Fig. 3. Any of the Antarctic scenarios for mwp-IA produce roughly equivalent sea-level variations at Barbados and the Sunda Shelf (Fig. 2) and are thus consistent with the observations. Other scenarios are also consistent with the Barbados and Sunda Shelf data (Fig. 2), but independent constraints (*14, 31*) suggest that they are less likely than an Antarctic-specific scenario.

This first application of the sea-level test to the Barbados and Sunda Shelf data suggests that the meltwater pulse did not originate solely from the southern margin of Laurentia (*32*) and that a substantial contribution may have originated from Antarctica (*33*). A final conclusion in this regard requires an improvement in the observational constraints at the Sunda Shelf across the mwp-IA interval. Moreover, this application, together with the results in Figs. 1 and 2, indicate that efforts to establish and refine bounds on sea-level change across mwp-IA at a suite of additional sites (including, for example, Tahiti and the Argentine Shelf) provide the key to determining the source of this enigmatic melting event.

References and Notes

1. B. D. Douglas, *J. Geophys. Res.* **96**, 6981 (1991).
2. E. Bard, B. Hamelin, R. G. Fairbanks, A. Zindler, *Nature* **345**, 405 (1990).
3. See (*34*) for a comprehensive review of observations and arguments related to this question.
4. W. R. Peltier, *Science* **265**, 195 (1994).
5. J. P. Kennett, N. J. Shackleton, *Science* **188**, 147 (1975).
6. A. Leventer, D. F. Williams, J. P. Kennett, *Earth Planet. Sci. Lett.* **59**, 11 (1982).
7. L. D. Keigwin, G. A. Jones, S. J. Lehman, E. A. Boyle, *J. Geophys. Res.* **96**, 16811 (1991).
8. R. G. Fairbanks, C. D. Charles, J. D. Wright, in *Radiocarbon After Four Decades*, R. E. Taylor, A. Long, R. S. Kra, Eds. (Springer-Verlag, New York, 1992), pp. 473–500.
9. J. T. Andrews, H. Erlenkeuser, K. Tedesco, A. E. Aksu, A. J. T. Jull, *Quat. Res.* **41**, 26 (1994).
10. L. D. Keigwin, G. A. Jones, *Paleoceanography* **10**, 973 (1995).
11. Some of these objections are as follows: (i) The size of the meltwater pulse would have required that the entire southern sector become an ablation zone and melt away at unprecedented rates. The geological evidence, however, clearly shows that ice remained throughout most of this region at the end of the event (*35*). (ii) It is difficult to explain how those sectors of the Laurentide Ice Sheet that drained to the Hudson Strait and the Gulf of St. Lawrence remained immune to a climate forcing that induced a nearby catastrophic melting event. (iii) Most ocean models (*36*), although not all (*37*), suggest that a freshwater flux of this magnitude derived from the Mississippi River would substantially reduce the Atlantic thermohaline circulation (THC) without delay. Proxy records of changes in the THC, however, show that mwp-IA occurred more than 1000 years before the next significant change in the THC associated with the Younger Dryas cold interval. (iv) The $\delta^{18}O$ anomaly in the Gulf of Mexico record shows that excursions of similar magnitude and sign occurred before mwp-IA, indicating that the anomalies may reflect relatively minor fluctuations in meltwater discharge down the Mississippi River (*34*).
12. D. R. Lindstrom, D. R. MacAyeal, *Nature* **365**, 214 (1993).
13. G. E. Birchfield, H. Wang, J. J. Rich, *J. Geophys. Res.* **99**, 12459 (1994).
14. Oxygen isotope records from both the Norwegian and Greenland Seas and reconstructed salinities for the northeastern North Atlantic indicate little, if any, meltwater discharge from either the Barents Sea or Fennoscandian Ice Sheets during mwp-IA (*34*). In addition, neither ice sheet appears to have been capable of delivering volumes sufficient to account for mwp-IA.
15. T. J. Hughes, in *The Geology of North America, Vol. K-3, North America and Adjacent Oceans During the Last Deglaciation*, W. F. Ruddiman, H. E. Wright Jr., Eds. (Geological Society of America, Boulder, CO, 1987), pp. 183–220.
16. E. Bard *et al.*, in *The Geological History of the Polar Oceans: Arctic Versus Antarctic*, U. Bleil, J. Thiede, Eds. (Kluwer Academic, Norwell, MA, 1990), pp. 405–415.
17. A. Shemesh, L. H. Burckle, J. D. Hays, *Paleoceanography* **10**, 179 (1995).
18. R. S. Woodward, *U.S. Geol. Surv. Bull.* **48**, 87 (1888).
19. W. E. Farrell, J. A. Clark, *Geophys. J. R. Astron. Soc.* **46**, 647 (1976).
20. J. X. Mitrovica, M. E. Tamisiea, J. L. Davis, G. A. Milne, *Nature* **409**, 1026 (2001).
21. M. Tushingham, W. R. Peltier, *J. Geophys. Res.* **96**, 4497 (1991).
22. G. A. Milne, J. X. Mitrovica, J. L. Davis, *Geophys. J. Int.* **139**, 464 (1999).
23. J. X. Mitrovica, W. R. Peltier, *J. Geophys. Res.* **96**, 20053 (1991).
24. For this purpose, we have adopted the seismic model PREM (preliminary reference Earth model) described in (*38*).
25. The neglect of thermal expansion effects in the present study contrasts with analyses of the geographic variation in present-day sea-level change driven by ongoing melting of polar ice complexes (*20, 39–42*). In this case, thermal expansion on the order of 1 mm/year (*43*) is comparable in amplitude to the observed rate of present-day global sea-level rise (*1*).
26. This is not to say that far-field data are immune to contamination from GIA. We quantify this contamination in (*32*) for the case of the differential sea-level change between Barbados and the Sunda Shelf across the mwp-IA event.
27. E. Bard *et al.*, *Nature* **382**, 241 (1996).
28. T. Hanebuth, K. Stattegger, P. M. Grootes, *Science* **288**, 1033 (2000).
29. M. Stuiver *et al.*, *Radiocarbon* **19**, 355 (1998).
30. The marker dated at 13,500 yr B.P. (solid red squares in Fig. 3), which defines the end of our analysis time window, is a wood sample collected more than 100 km from other Sunda Shelf data. Hence, our estimate of a sea-level rise of 25 m from 14,200 yr B.P. to 13,500 yr B.P. at this site is dependent on the veracity of a composite sea-level curve. Furthermore, the sea-level variation just before mwp-IA is not well resolved on the Sunda Shelf curve.
31. In the case of a southern Laurentian source for mwp-IA, a sea-level rise of 25 m at Barbados would also be accompanied by a sea-level rise of 43 m at Tahiti. From Fig. 3, sea level at Tahiti subsequent to mwp-IA was ~ –80 m (*27*). For the southern Laurentian scenario, we would thus infer a sea level at Tahiti, just before the onset of mwp-IA, of ~ –123 m. The large discrepancy between this value and the observed contemporaneous sea level at other far-field sites (e.g., Fig. 3) is also an argument, albeit indirect, against this specific scenario. The same argument applies to the scenarios involving all Northern Hemisphere ice sheets (North-ICE3G) and all global ice sheets (All-ICE3G).
32. This conclusion is relatively insensitive to the sea-level signal as a result of ongoing GIA across the mwp-IA time window. We performed GIA calculations in which we predicted sea-level changes during a 1000-year period beginning at 14,500 yr B.P. that were driven by late Pleistocene glaciation/deglaciation events before the meltwater pulse. GIA calculations are commonly based on spherically symmetric, viscoelastic Earth models that are specified by values for the upper and lower mantle viscosity (where the boundary between the two regions is taken to be 670 km depth) and the thickness of the elastic lithosphere. We varied each of these three parameters over a broad range of possible values and found that the differential sea-level rise (Barbados minus Sunda Shelf) was no greater than 1.8 m. This bound takes into account that the sea-level marker dated to 13,500 calendar yr B.P. at the Sunda Shelf is significantly displaced geographically relative to older markers on the same curve (*30*).
33. There are several important implications if the meltwater pulse originated largely from Antarctica: (i) It indicates that substantial deglaciation occurred several thousand years before the onset of Antarctic deglaciation suggested from ice sheet and GIA models [see discussion in (*34*)]. (ii) If substantial ice is required in Antarctica after mwp-IA to account for the younger deglaciation phase predicted by these models, then the excess, pre–mwp-IA ice may resolve the discrepancy between total ice volumes during the last glacial maximum reconstructed from ice sheet models and from some GIA models (*44*). (iii) An Antarctic source would resolve the apparent conundrum of having a large freshwater forcing in the North Atlantic with a 1000-year delay in the response of the Atlantic THC (*11*).
34. P. U. Clark *et al.*, *Paleoceanography* **11**, 563 (1996).
35. A. S. Dyke, V. K. Prest, *Geogr. Phys. Quat.* **41**, 237 (1987).
36. S. Manabe, R. J. Stouffer, *Paleoceanography* **12**, 321 (1997).
37. K. Sakai, W. R. Peltier, *J. Geophys. Res.* **100**, 13455 (1995).
38. A. M. Dziewonski, D. L. Anderson, *Phys. Earth Planet. Inter.* **25**, 297 (1981).
39. J. A. Clark, J. A. Primus, in *Sea-Level Changes*, M. J. Tooley, I. Shennan, Eds. (Institute of British Geographers, London, 1987), pp. 356–370.
40. S. M. Nakiboglu, K. Lambeck, in *Glacial Isostasy, Sea-Level and Mantle Rheology*, R. Sabadini, K. Lambeck, E. Boschi, Eds. (Kluwer Academic, Dordrecht, Netherlands, 1990), pp. 237–258.
41. C. Conrad, B. H. Hager, *Geophys. Res. Lett.* **24**, 1053 (1997).
42. H.-P. Plag, H.-U. Jüttner, *Mem. Natl. Inst. Polar Res.* (special issue 54), 301 (2001).
43. C. Cabanes, A. Cazenave, C. Le Provost, *Science* **294**, 840 (2001).
44. P. U. Clark, A. C. Mix, *Quat. Sci. Rev.* **21**, 1 (2002).
45. E. Bard, M. Arnold, R. G. Fairbanks, B. Hamelin, *Radiocarbon* **35**, 191 (1993).
46. R. G. Fairbanks, *Nature* **342**, 637 (1989).

47. Supported by the NSF Earth System History program (P.U.C.), the Canadian Institute for Advanced Research (J.X.M.), PREA funding from the Government of Ontario (J.X.M., M.E.T.), the Natural Sciences and Engineering Research Council of Canada (J.X.M.), and a McLean Research Award from the University of Toronto (J.X.M.). We thank M. Ishii for assistance in preparing Fig. 2.

7 December 2001; accepted 15 February 2002